Performance analysis of three sides solar air heater having roughness elements as a combination of multiple-v and transverse wire on the absorber plate

DHANANJAY KUMAR[*]
LALJEE PRASAD

National Institute of Technology, Jamshedpur Jharkhand 831014, India

Abstract   Artificial roughness has been found to enhance the thermal performance from the collector to air in the solar air heater duct. This paper presents the results of experimental investigation on thermal performance of three sides solar air heater roughened with combination of multiple-v and transverse wire. The range of variation of system and operating parameters is investigated within the limits of relative roughness pitch of $10-25$, relative roughness height of $0.018-0.042$, angle of attack of $30°-75°$ at varying flow Reynolds number in the of range of $3000-12000$ for fixed value of relative roughness width of 6. The augmentation in fluid temperature flowing under three side's roughened duct is found to be 36.57% more than that of one side roughened duct. The maximum thermal efficiency is obtained at relative roughness pitch of 10 and relative roughness height of 0.042, and angle of attack of $60°$. The augmentation in thermal efficiency of three sides over those of one side roughened duct is found to be $46-57\%$ for varying values of relative roughness pitch, $38-50\%$ for varying values of relative roughness height, and $40-46\%$ for varying values of angle of attack.

Keywords: Reynolds number; Relative roughness height; Relative roughness pitch; Solar air heater; Thermal efficiency; One side roughened duct; Three side's roughened duct

---

[*]Corresponding Author. Email: dhananjaykumar84nit@gmail.com

Nomenclature

A_p	–	surface area of absorber plate, m^2
A_o	–	area of orifice plate, m^2
H	–	height of the duct, m
C_p	–	specific heat of air at constant pressure, J/kgK
D_h	–	hydraulic diameter of solar air heater, $(= 4WH/2(W + H))$, m
e	–	artificial roughness height, m
Δh_1	–	height of U-tube manometer fluid column, m
Δh_2	–	height of micromanometer fluid column, m
I	–	intensity of solar radiation W/m^2
L	–	length of test section, m
$\dot{m}$	–	mass flow rate of air, kg/s
P	–	roughness pitch, m
ΔP_o	–	pressure difference of manometeric fluid level in U-tube manometer, Pa
ΔP_d	–	pressure difference of water column level in micromanometer, Pa
Q_u	–	useful heat gain, W
ΔT	–	temperature difference of fluid, K
t_a	–	ambient temperature, K
t_o	–	outlet temperature of fluid, K
t_i	–	inlet temperature of fluid, K
t_{pm}	–	mean plate temperature, K
t_{fm}	–	mean fluid temperature, K
W	–	width of duct, m

Dimensionless parameters

e/D_h	–	relative roughness height
$\eta_{th(3r)}$	–	thermal performance for three sides rough
$\eta_{th(1r)}$	–	thermal performance for one side rough
P/e	–	relative roughness pitch
W/H	–	duct aspect ratio
Re	–	Reynolds number
W/w	–	relative roughness width
d/w	–	relative gap position
η_R	–	thermal efficiency ratio

Greek symbols

η, η_{th}	–	thermal efficiency
ρ	–	density of air kg/m^3
ρ_1	–	density of fluid used in U-tube manometer, kg/m^3
ρ_2	–	density of fluid used in micromanometer, kg/m^3
α	–	angle of attack, degree
β	–	ratio of orifice to pipe diameter
$1r$	–	one side rough
$3r$	–	three sides rough

1 Introduction

The increasing gap between demand and supply as well as high cost of energy have resulted in increased efforts to design more efficient heat exchangers and for this purpose several viable engineering solutions are available, particularly with the use of heat transfer enhancement methods. Joule (1861) first attempted to enhance heat transfer coefficients in condensing steam about 158 years ago and since then it continues to be a major research and development activity [1, 2, 22–30]. In solar energy applications, solar air heater is the most simple and commonly used heat exchanger device to convert the incoming solar radiations into thermal energy, which is extracted by air flowing under the absorbing surface. The schematic diagram of conventional solar air heater has been shown in Fig. 1. However, the formation of laminar sublayer over the heat-transferring surface impedes the heat transfer to the flowing air, thereby, adversely affecting the thermal performance of solar air heaters. In order to improve the heat transfer in solar air heaters, use of artificial roughness on the surface is an effective technique to enhance the heat transfer to fluid flowing in the duct. Artificial roughness in the form of repeated wires is used to disturb the laminar sublayer and create local wall turbulence. Contrary to this, the excessive disturbance to the boundary layer creates more friction resulting in more pumping power. Therefore, the turbulence must be created in the region of laminar sub layer. The use of wires is one of the most desirable methods on account of their ability to combine heat transfer coefficient enhancement
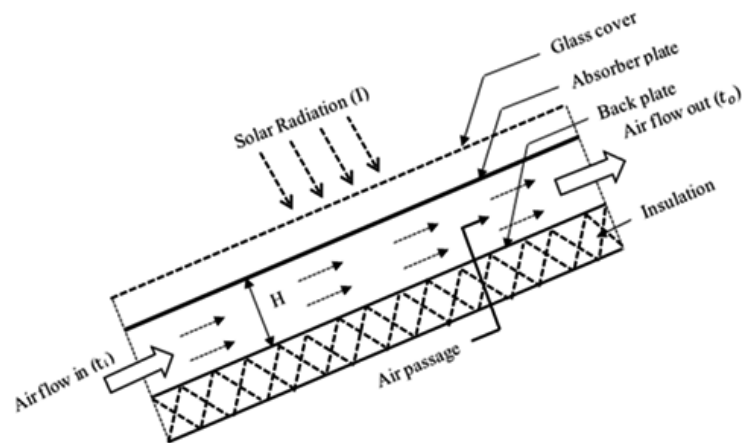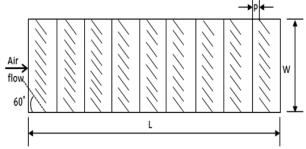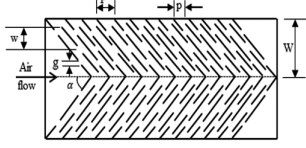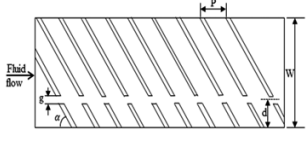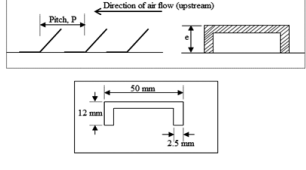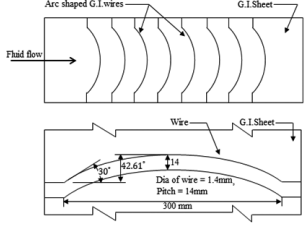

Figure 1: Schematic diagram of conventional solar air heater.

with limited frictional losses. The use of artificial roughness in solar air heaters owes its origin to several investigations carried out in connection with the enhancement of heat transfer in nuclear reactors, cooling of turbine blades and electronic equipment [3–5, 31–35]. Prasad and Mullick [6], Gupta [7], Saini and Saini [8] and Karwa [9] have carried out investigations on rib roughened absorber plates of solar air heaters that form a system with only one roughened wall and three smooth walls. Correlations for heat transfer coefficient and friction factor have been developed for such systems. However, the increase in heat transfer is accompanied by an increase in the resistance of fluid flow. The application of artificial roughness in the form of fine wires on the heat transfer surface has been recommended to enhance the heat transfer coefficient by several investigators. Prasad and Mullick used artificial roughness in the form of fine wires in a solar air heater duct to improve the thermal performance of collector and they have obtained the enhancement (ratio of the values for roughened duct to that for the smooth duct) in Nusselt number of the order of 1.385 [6]. Gupta found that the heat transfer coefficient of roughened duct using wires as artificial roughness can be improved by a factor up to 1.8 and the friction factor has been found to increase by a factor up to 2.7 times of smooth duct [7]. Saini and Saini reported that a maximum enhancement in Nusselt number and friction factor for a duct roughened with expanded metal mesh is of the order of 4 and 5 respectively in the range of parameters investigated [8]. Karwa concluded that considerable enhancement of heat transfer can be obtained as a result of providing rectangular or chamfered rib roughness on the heat transferring surface of a rectangular section duct [9]. The Stanton number has been found to increase by about $1.5 - 1.8$ times for $W/H = 4.82$ and $e/D_h = 0.029$ and $1.7 - 2.1$ times for $W/H = 7.75$ and $e/D_h = 0.044$ for $\text{Re} > 8$ as compared to smooth duct. The corresponding values of increase in friction factor are $2 - 2.7$ times and $2.9 - 3.1$ times respectively. Prasad and Saini reported that a maximum enhancement in Nusselt number and friction factor which are 2.38 and 4.25 times of smooth duct has been obtained by using artificial roughness [10]. Cortes and Piacentini have reported that incorporating wire-type periodic perturbations on the absorber plate of solar air heater enables efficiency improvements of $9 - 55\%$ to be attained over the studied range of situations [11]. Although the heat transfer problems can be investigated by analytical means too, but due to the complex nature of governing equations and the difficulty in obtaining analytical/numerical solutions, the researchers have focused greater attention on the experimental investigation. Sufficient information

is available in the literature about heat transfer and friction characteristics for flow in roughened circular tubes and channels in the turbulent flow. The roughness wire orientation and geometry, i.e., relative roughness pitch and relative roughness height, strongly affects the flow structure [12, 13]. Different roughness geometries are shown in Tab. 1.

Table 1: Different roughness geometry used in solar air heaters.

Authors	Range of roughness parameters	Roughness geometry
1. Varun *et al.* [13] (Inclined broken ribs)	$P/e = 3-8$ $e/D_h = 0.030$ Re $= 2000-14000$	
2. N.S. Deo *et al.* [14] (Multi-gap v-down combined with staggered ribs.)	$P/e = 6-12$ $e/D_h = 0.026-0.057$ $\alpha = 40°-80°$ $g/e = 1$ $w/e = 4.5$ $p/P = 0.65$ Re $= 4000-12000$	
3. Kumar *et al.* [15] (Inclined broken ribs)	$P/e = 8-16$ $e/D_h = 0.0249-0.0498$ $d/w = 0.15-0.3$ $g/e = 1$ Re $= 4105-20526$	
4. Bopche and Tandale [16] (U-shaped ribs)	$P/e = 6.67-57.14$ $e/D_h = 0.0186-0.03986$ Re $= 3800-18000$ $\alpha = 90°$	
5. Saini and Saini [17] (Arc shape roughness)	$P/e = 10$ $e/D_h = 0.0213-0.0422$ $\alpha/90 = 0.3333-0.6666$ Re $= 2000-17000$	

In the present experimental investigation, a combination of multiple-v and transverse wires used as roughness geometry on the absorber plate is taken, the range of parameters covered are: Reynolds number, Re = 3000−12000; relative roughness pitch, $P/e = 10−25$; relative roughness height, $e/D_h = 0.018−0.042$; angle of attack, $\alpha = 30°−75°$ and fixed value of relative roughness width, $W/w = 6$; with the duct aspect ratio, $W/H = 8$ as shown in Tab. 2.

Table 2: Values of roughness and flow parameters.

No.	Parameter	Values
1.	Relative roughness pitch (P/e)	10−25 (4 levels)
2.	Relative roughness height (e/D_h)	0.018−0.042 (4 levels)
3.	Angle of attack α	30°−75°(4 levels)
4.	Relative roughness width (W/w)	6 One (level)
5.	Reynolds number (Re)	3000−12000 (6 levels)

The main objectives of the present investigation are:

1. To develop such solar air heater and carry out experiments under actual outdoor conditions and collect various sets of experimental data for one side as well as three sides' roughened solar air heater ducts.

2. To reduce the experimental data in such solar air heaters and compare the thermal performance of the proposed roughness pattern with three sides roughened and other best performing of the multiple-v rib roughness one side solar air heater as reported by Hans *et al.* [20].

3. To study the effect of relative roughness pitch, relative roughness height and angle of attack at varying values of flow Reynolds number on thermal performance of solar air heater roughened on three sides (top wall multiple-v and two side wall transverse wire) solar air heaters and find best performing parameters.

2   Experimental set-up and experimentation

The test set-up used for experimentation in the present work has been fabricated as per the guidelines of ASHRAE Standard 93–77 (1977) for testing roughened solar collectors under actual outdoor conditions using

the open loop system [18]. The schematic diagram of the experimental set-up has been shown in Fig. 2. The experimental set-up has been developed with quality of plywood and wooden boards. The setup is accommodated with three ducts parallel to each other, namely X, Y, and Z as shown in Fig. 3. The present experimental investigation employs the duct X and Z containing one side and three sides' roughened solar collector respectively. Each solar air heater duct setup is 2000 mm long, 200 mm wide and 25 mm height, only 1500 mm of the duct length act as the test section and remaining 500 mm as the flow stabilization bell mounted entry section. The solar collector entry section was prevented from the solar radiation and insulated. Artificial roughness has been provided on the fluid flow side of the absorber plate, for one side roughened duct, roughness is provided on the top side serving as absorber plate, two side walls are insulated and 4 mm thick glass cover is on the top side and the bottom is insulated by means of wooden plywood. For three side's roughened duct, roughness is provided to the three sides, i.e., on top and two side walls of the absorber plate (top wall
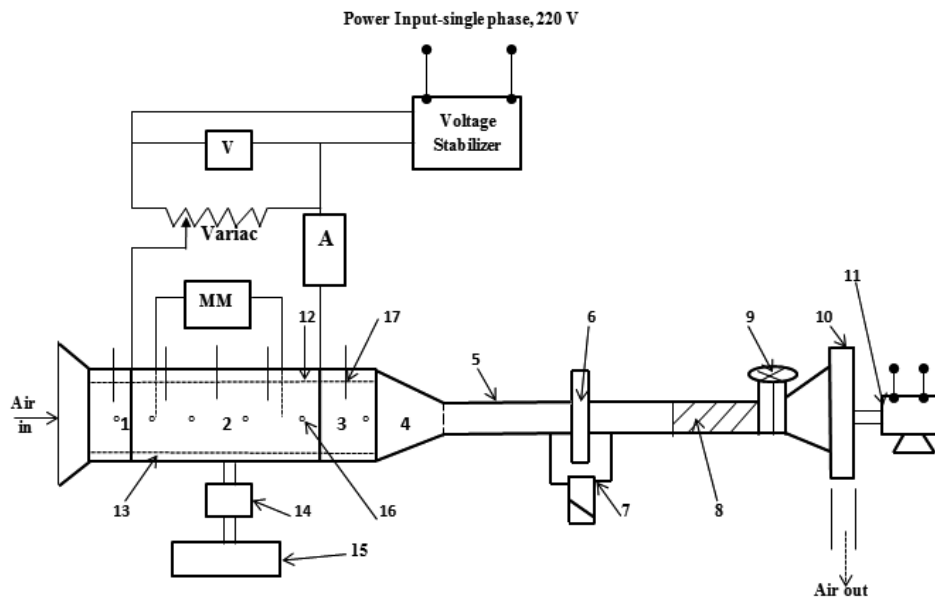

Figure 2: Schematic diagram of the experimental set-up: 1 – unheated entry section, 2 – heated test section, 3 – exit section, 4 – transition section, 5 – flow pipe, 6 – orifice meter, 7 – inclined U-tube manometer, 8 – flexible pipe, 9 – gate valve, 10 – blower, 11 – electric motor, 12 – absorber plate, 13 – bottom of duct, 14 – selectors switch 15 – temperature recorder, 16 – thermocouple, 17 – digital thermometer, A – ammeter, V – voltmeter, MM – micromanometer.

multiple-v and two side walls transverse wire) as shown in Fig. 4. Three
sides roughened duct contains three side glass covers and bottom sides are
insulation. The height of roughness element is very small (remains limited
to sub-layer thickness) at various values of pitch and side of the duct are
small (for high values of aspect ratio in case of solar air heaters, i.e., for
$W \gg B$, providing artificial roughness element in the duct negligibly effect
the flow area of the three sides roughened duct may be considered equal to
that of one side roughened duct.

Figure 3: Photograph of the experimental set-up.

Figure 4: Photograph of absorber plates.

The two ducts used in the experimental setup are similar in all terms of
dimensions and orientation so that heat transfer and thermal performance
characteristics can be directly compared. The absorber plates are painted
black to absorb maximum possible incident solar radiation. The set-up is

sealed using lightly moistened putty and m-seal to ensure air tight setup. Calibrated copper constantan thermocouples of 28 SWG (British Standard Wire Gauge) were used for measuring the plate temperature. Eighteen numbers of thermocouples are used to measure the plate temperature whose output is given by a digital voltmeter assembled in the setup. Six thermocouples are placed on the top absorber plate of one side roughened duct and rest twelve thermocouples are placed on three sides roughened duct (six on top and six on side walls). Digital thermometers are used to measure the air temperature at six locations along the ducts. A blower was used to suck the air to flow through the roughened ducts. The desired flow rate of air through the duct was regulated using an auto variac. A digital pyranometer, powered by a solar panel as shown in Fig. 5 measured the intensity of solar radiation. Multitube manometers were connected to the pressure taps provided in the test section in both the ducts for measuring the pressure drop, and mass flow rate was measured by means of a flange-tap orifice-meter fitted in flow pipe.

Figure 5: Photograph of digital pyranometer.

Test data were collected for 12 sets of the roughened absorber plate and 60 test runs for both one side and three sides artificially roughened solar air heaters. The entire experimental work can be carried out under actual outdoor conditions. For a single day, data were collected for a given value of mass flow rate under varying values of intensity of solar radiation within intervals of 15 min between 11:00 a.m. to 02:00 p.m. on clear sky day.

The value of the hydraulic diameter for both the solar air heater ducts is worked out to be 44.44 mm, as the ducts are kept similar in dimensions.

3   Data reduction

The experimental data for plate and air temperatures at various locations in the duct was recorded under steady state conditions for a given heat flux and mass flow rate of air. Following equations have been used for evaluation the numerical values of experimental observations as described below.

The mass flow rates have been determined from the pressure drop measurement across the orifice plate

$$\dot{m} = C_d A_o \left[\frac{2\rho \Delta P_o}{1 - \beta^4} \right]^{0.5}, \tag{1}$$

where

$$\Delta P_o = 9.81 \rho_1 \Delta h_1 \sin \theta. \tag{2}$$

Calibration of orifice plate against a standard Pitot tube yielded a value of 0.624 for coefficient of discharge (C_d).

The useful heat gain by air and heat transfer coefficient (h) for one side and three sides artificially roughened collectors can be determined by formula

$$Q_u = \dot{m} C_p (t_o - t_i) = h A_p (t_{pm} - t_{fm}). \tag{3}$$

Collector area for three sides roughened absorber plate can be calculated using the expression

$$A_{p(3r)} = LW + 2LH, \tag{4}$$

where L, H, and W are length, height and width of the absorber plate respectively.

The mean temperature of the absorber plate has been calculated based on readings of digital voltmeter that reads the output of thermocouples placed on six different locations of the absorber plate as

$$t_{pm} = \frac{t_{pr1} + t_{p2} + t_{p3} + t_{p4} + t_{p5} + t_{p6}}{6}. \tag{5}$$

The mean temperature of the fluid can be calculated based on output reading temperature of digital thermometers placed on six different locations of the absorber plate as

$$t_{fm} = \frac{t_{f1} + t_{f2} + t_{f3} + t_{f4} + t_{f5} + t_{f6}}{6}. \tag{6}$$

Hydraulic diameter

$$D_h = \frac{4WH}{2(W+H)}.$$ (7)

The thermal efficiency of artificially roughened solar air heater is defined as the ratio of useful heat gain (Q_u) per unit area of the absorber plate to the incident thermal radiation and is calculated as

$$\eta = \frac{Q_u}{IA_p},$$ (8)

where I is intensity of solar radiation. The area of absorber plate A_p (area of heat transfer) is different for one side and three sides roughened. For the case of one side roughened it is equal to the product of length and width, while three side roughened one is determined by Eq. (4).

4 Uncertainty analysis

Uncertainties in final experimental results have been calculated based upon the analysis of errors incurred by experimental measurements with various instruments. The uncertainty analysis has been done using the method given by the following equation [19].

$$U_x = \left[\left(\frac{\partial X}{\partial y_1} U_{y1} \right)^2 + \left(\frac{\partial X}{\partial y_2} U_{y2} \right)^2 + \ldots + \left(\frac{\partial X}{\partial y_n} U_{yn} \right)^2 \right]^{0.5},$$ (9)

where $y_1, y_2, \ldots, y_n$ are the variables effecting the parameters X and U stands for uncertainty.

The most important parameters in this present work are the thermal efficiency calculated by the equation

$$\eta = \frac{\dot{m}C_p (t_o - t_i)}{A_p I} = \frac{\dot{m}C_p \Delta T}{A_p I}.$$ (10)

From Eqs. (9) and (10), uncertainty in the thermal efficiency of solar air heater is given by

$$U_\eta = \left[\left(\frac{C_p \Delta T}{A_p I} U_{\dot{m}} \right)^2 + \left(\frac{\dot{m} \Delta T}{A_p I} U_{c_p} \right)^2 + \left(\frac{\dot{m}}{A_p I} U_{\Delta T} \right)^2 \right.$$

$$\left. + \left(\frac{\dot{m}C_p \Delta T}{A_p^2 I} U_{A_c} \right)^2 + \left(\frac{\dot{m}C_p \Delta T}{A_p I^2} U_I \right)^2 \right]^{0.5},$$ (11)

where $U_{\dot{m}}$, U_{c_p}, $U_{\Delta T}$, U_{A_p}, and U_I are the uncertainties in mass flow rate of air, specific heat of air, air temperature rise, area of absorber plate and intensity of solar radiation, respectively. The respective values of uncertainty in $U_{\dot{m}}$, U_{c_p}, $U_{\Delta T}$, U_{A_p}, and U_I, for a particular test run being 2.01155×10^{-9}, 0, $0.15°$, 1.52137×10^{-3} and 0, when substituted in Eq. (11), result in the thermal efficiency uncertainty of 1.35%.

5 Result and discussion

Rigorous experimental work has been performed and data for both three sides roughened and one side roughened ducts have been recorded simultaneously at varying values of the flow Reynolds number. For three sides roughened solar air heaters having combination of multi-v and transverse wire (top wall multi-v and two side walls transverse) with investigation parameters, at relative roughness pitch, P/e in the range of $10-25$; relative roughness height, e/D_h in the range of $0.018-0.042$; angle of attack, α varied from $30°-75°$, have been tested and compared to the results over one side roughened (fixed absorber plate) solar air heater ducts with relative roughness pitch, P/e of 10; relative roughness height, e/D_h of 0.042 and angle of attack, $\alpha = 60°$ for fixed values of relative roughness width, W/w of 6. Data has been collected for six different values of mass flow rates for each duct with specific roughness elements. The entire experimental investigation is carried out under actual outdoor conditions for which measurements were the pressure drop across orifice meter, pressure drop across the duct, temperature along the absorber plate, air temperature at the inlet and the outlet of the ducts and the intensity of incident solar radiation. During a particular day intensity of solar radiation varied from 729 to 886 W/m^2 and ambient temperature varied from $33.8\,°$C to $38.8\,°$C. Values of some typical recorded data are shown in Tab. 3.

5.1 Variation in ambient conditions

Figure 6 shows the variation of intensity of solar radiation and ambient temperature on a typical day with respect to time during the experimental period ranging from 11:00 a.m. to 02:00 p.m. It is clear from the figure as the day progresses; the intensity of solar radiation increases remarkably up to 11:30 hr, when after it decreases periodically. As far as the ambient temperature is concerned, it increases monotonously. It is found that

Table 3: Values of some metrological data.

Metrological parameters	Units	Time (h)												
		11:00	11:15	11:30	11:45	12:00	12:15	12:30	12:45	13:00	13:15	13:30	13:45	14:00
Ambient temperature	$^\circ$C	33.8	34.4	34.33	35.43	36.1	36.4	36.6	37.2	37.4	38.8	38.2	38.5	38.56
Wind speed	m/s	4.7	1.9	4.4	1.8	2.2	2.1	3.3	1.5	4.5	2.4	4.6	2.0	2.5
Atmospheric pressure	1×10^2 N/m^2	983.2	982.9	982.9	982.7	982.5	982.3	982.1	981.7	981.3	980.9	980.7	980.3	980.3
Global radiation	W/m^2	857	878	886	877	868	860	850	822	803	767	763	739	729
Diffuse radiation	W/m^2	399	397	406	405	404	397	401	399	394	387	391	404	729
Direct radiation	W/m^2	453	470	461	454	452	453	448	435	433	411	406	378	345
Normal radiation	W/m^2	464	484	481	472	467	466	458	439	435	416	414	385	365
Relative humidity	%	48	48	48	48	48	48	46	46	41	41	36	35	32

the maximum value of solar radiation intensity is 886 W/m^2 and ambient temperature is 38.8°C on a particular day.
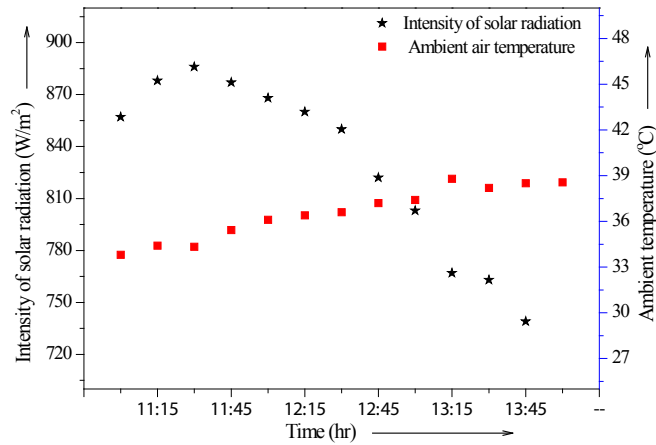

Figure 6: Variation of intensity of solar radiation and ambient air temperature during a day.

5.2   Plate and air temperature along test length

Figure 7 shows the variation in plate and air temperature for three sides and one side artificially roughened solar collector along the test length. It
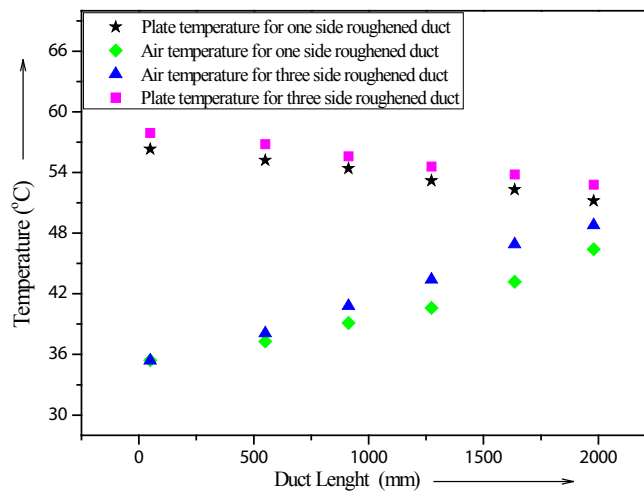

Figure 7: Variation of plate and fluid temperature.

can be observed that the rise in fluid temperature for three sides' roughened duct is higher as compared to one side roughened duct along the test length of the collector. Meanwhile, for plate temperature, three sides roughened duct experiences more temperature rise than that of one side roughened duct due to minimal heat transfer to the under flowing fluid (air) along the test length of the collector. From the figure it is clear that plate temperature and fluid temperature both are higher in three side's roughened collector than those of one side roughened collector and also observed that plate temperature decreases and fluid temperature increases along the test length of the collector.

5.3   Validation of experimental set-up

Validation of experimental thermal efficiency is determined for roughened solar air heater duct of multi-v, with fixed value of relative roughness pitch, $P/e = 10$; relative roughness height, $e/D_h = 0.042$; relative roughness width, $W/w = 6$ and angle of attack, $\alpha = 60°$. The respective values are calculated from best performing one side roughened solar air heater of Hans et al. [20] using correlation from mathematical model developed by Kumar and Prasad [21], and shown in Fig. 8. It is clear from the given figure the variation of thermal efficiency for both three sides and one side roughened duct from which it can be concluded that three sides roughened duct are
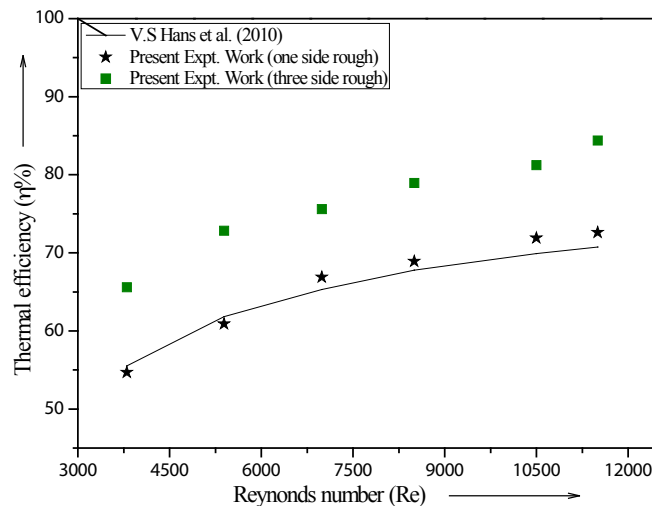

Figure 8: Validation of experimental work for thermal efficiency.

far more superior than those of one side roughened duct in terms of thermal performance. The percentage mean deviation of thermal efficiency for one side roughened duct was found to be $\pm 3.6\%$. The augmentation in the value of thermal efficiency for three sides roughened duct when compared to one side roughened duct was found to be in the range of $30-60\%$. This shows good agreement between experimental and theoretical values, which ensures the accuracy of the data collected with experimental set-up.

5.4   Thermal performance

On the basis of present experimental investigations, a comprehensive study of thermal performance of three sides roughened solar air heater having combination of multiple-v and transverse wire has been carried out for a wide range of flow and geometrical parameters. The results are shown in Figs. 9, 10, and 11 as thermal efficiency versus flow Reynolds number. The Reynolds number has been varied from 3000 to 12000. The relative roughness pitch, P/e has been varied from $10-25$. The relative roughness height, e/D_h has been varied from $0.018-0.042$, and for multiple-v angle of attack, α varied from $30^\circ - 75^\circ$. From the respective figure it is found that an increasing the value of flow Reynolds number, the thermal efficiency of both three sides and one side roughened solar air heater duct increases.
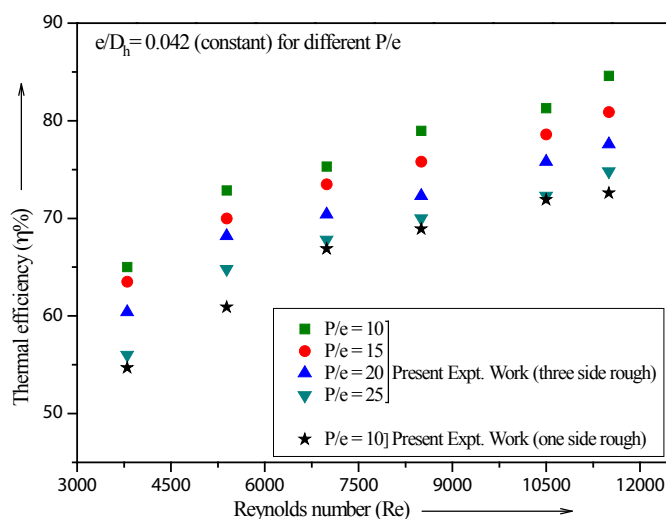

Figure 9: Thermal efficiency versus Reynolds number at varying relative roughness pitch (P/e).

Apart from the top absorber plate, providing roughness to both the side walls of the roughened duct in case of three sides roughened solar air heater enhances the useful heat gain of the under flowing fluid reducing absorber plate temperature that results in reduced heat loss from the roughened surface. At higher value of flow Reynolds number (Re > 12000) there is not much difference between thermal performance of one side and three sides roughened duct. This is due to the fact that at higher mass flow rates, air travels quickly inside the roughened duct and it does not get sufficient time to get affected by the roughness provided inside the duct.

Figure 9 reveals that thermal performance increases with decrease of relative roughness pitch, due to reduction of the distance of the reattachment point, breakup of the laminar sub-layer and creation of local wall turbulence. As a result the thermal resistance reduces and the heat transfer rate enhances greatly. The maximum thermal efficiency occurs at P/e values of 10, and rise in thermal performance of three sides over one side roughened solar air heater duct under varying values of relative roughness pitch is found to be $46-57\%$.

Thermal efficiency increases with increase of relative roughness height as shown in Fig. 10; at higher height of roughness created is more turbulence to the flow of air inside the duct, resulting in higher rate of heat transfer as compared to smaller height of roughness. The maximum thermal efficiency
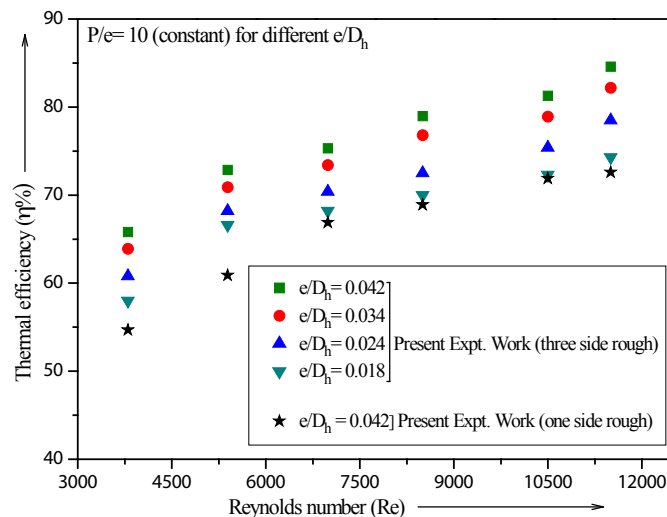

Figure 10: Thermal efficiency versus Reynolds number at varying relative roughness height $(e/D_h.)$

occurs at e/D_h values of 0.042 and rise in thermal efficiency of three sides roughened solar air heater duct under varying values of relative roughness height is found to be $38-50\%$ over that of one side roughened duct.

Figure 11 shows that the thermal efficiency is at maximum corresponding to values of angle of attack, $\alpha = 60°$ and thermal efficiency is lower at other values of angle of attack. The strength of secondary flow across the rib roughness changes with the change of angle of attack α rendering the variation in heat transfer thereby, the thermal efficiency caused by interaction of secondary-flow along the rib and boundary layer on the flow downstream sides of the wire rib. The possible reason that thermal efficiency is at maximum for values of angle of attack, $\alpha = 60°$ is that the separation of secondary flow due to presence of roughness element (inclination at this values) and the movement of vortices combining together, maximum occurs at this values of attack, and rise in thermal efficiency of three sides over that of one side roughened solar air heater duct is found to be $40-46\%$ under varying values of angle of attack.
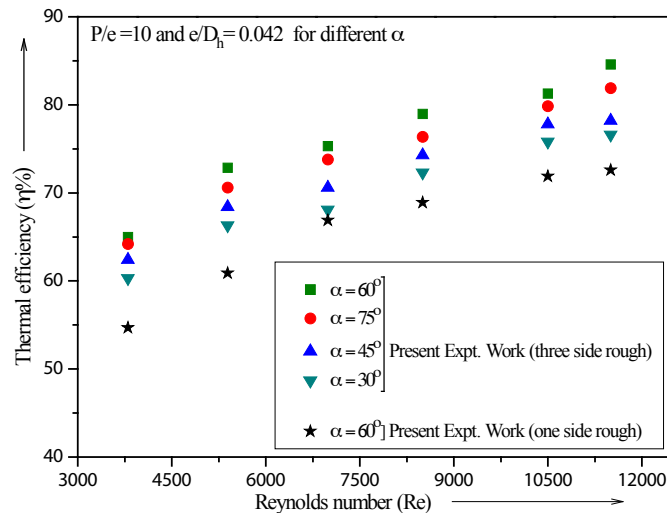

Figure 11: Thermal efficiency versus Reynolds number at varying angle of angle of attack (α).

5.5   Thermal efficiency ratio

The variation of thermal efficiencies enhancement ratio $\eta_{th(3r)}/\eta_{th(1r)}$ of three sides roughened to one side roughened solar air heater duct with the

Reynolds number for different values of relative roughness height (e/D_h), for fixed value of relative roughness pitch, $P/e = 10$ and angle of attack, $\alpha = 60°$ has been shown in Fig. 12. It is found that the ratio η_R is highest for highest value of relative roughness height and is the lowest for lowest value of relative roughness height; however this trend of variation for all values of e/D_h is the same. The Reynolds number corresponding to the maximum thermal efficiency enhancement ratio (η_R) shifts towards lower values of Reynolds number as e/D_h increases.
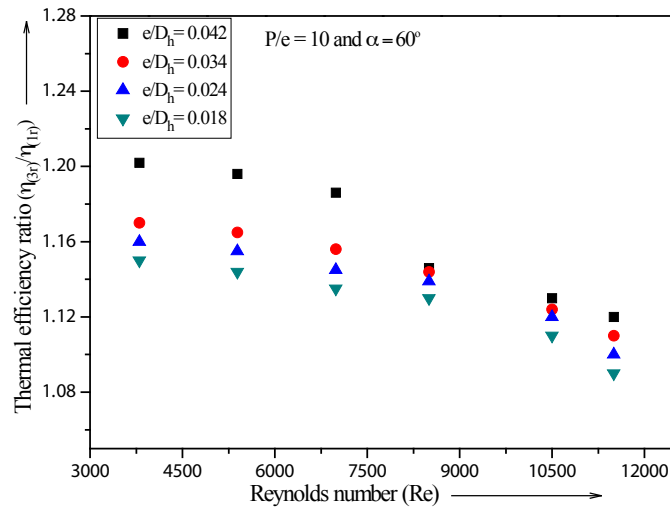

Figure 12: Thermal efficiency ratio versus Reynolds number.

6 Conclusions

Based upon the experimental investigation results in terms of thermal performance regarding the effect of flow Reynolds number, relative roughness pitch, relative roughness height and angle of attack on solar air heater roughened with combination of multiple-v and transverse wire can be listed as given below:

1. The entire experimental investigation is carried out under actual outdoor conditions in which solar insolation varied from 729 to 886 W/m^2 during the day. Useful heat gain by the flowing air under the absorber plate, the air temperature from inlet to outlet increases while plate

temperature from inlet to outlet decreases. The standard mean deviation of thermal performance results for present experimental work compared to best performing experimental work carried out by Hans *et al.* [20] is found to be $\pm 3.6\%$. The cause for such deviation has been accounted as variation in ambient condition like solar radiation, wind speed, ambient temperature, convective heat transfer coefficient, specific heat capacity of air etc., and also uncertainty in measurements.

2. The augmentation of air temperature in three sides over that of one side roughened solar air heater is found to be 36.67% at relative roughness pitch value of 10; relative roughness height value of 0.042 and angle of attack of $60°$.

3. The enhancement of thermal efficiency due to implementation of artificial roughness having combination of multiple-v and transverse wire shape on the absorber plate in three side's roughened solar air heater ducts is found to more than that of one side roughened duct. The enhancement in thermal performance are found to be $46-57\%$ for varying values of relative roughness pitch, $38-50\%$ for varying values of relative roughness height and $40-46\%$ for varying values of angle of attack.

4. The efficiency ratio of thermal performance is higher at lower mass flow rates, which is attributed to the increase in the value of the convective heat transfer coefficient due to the provision artificial roughness.

References

[1] BERGLES A.E.: *ExHFT for fourth generation heat transfer technology.* Exp. Therm. Fluid Sci. **26**(2002), 4, 335–344.

[2] BERGLES A.E.: *New frontiers in enhanced heat transfer advances in enhanced heat transfer.* In: Manglik, R.M. *et al.* (Eds.). ASME, New York, NY, (2000), 1–8.

[3] HAN J.C., ZHANG Y.M., LEE C.P.: *Augmented heat transfer in square channels with parallel, crossed and V-shaped angled ribs.* J. Heat Trans-T. ASME **113**(1991), 3, 590–596.

[4] HAN J.C., ZHANG Y.M.: *High performance heat transfer ducts with parallel broken and V-shaped broken ribs.* Int. J. Heat Mass Tran. **35**(1992), 2, 513–523.

[5] Wright L.M., Fu W.L., Han J.C.: *Thermal performance of angled, V-shaped and W-shaped rib turbulators in rotating rectangular cooling channels ($AR = 4$:1).* J. Turbomach. **126**(2004), 4, 604–614.

[6] Prasad K., Mullick S.C.: *Heat transfer characteristics of a solar air heater used for drying purposes.* Appl. Energy **13**(1983), 2, 83–93.

[7] Gupta D.: *Investigations on fluid flow and heat transfer in solar air heaters with roughened absorbers.* PhD thesis. University of Roorkee, 1993.

[8] Saini R.P., Saini J.S.: *Heat transfer and friction factor correlations for artificially roughened ducts with expanded metal mesh as roughness element.* Int. J. Heat Mass Tran. **40**(1997), 4, 973–986.

[9] Karwa R.: *Investigation of thermo-hydraulic performance of solar air heaters having artificially roughened absorber plate.* PhD thesis, University of Roorkee,1997.

[10] Prasad B.N., Saini J.S.: *Effect of artificial roughness on heat transfer and friction factor in a solar air heater.* Sol. Energy **41**(1988), 6, 555–560.

[11] Cortes A., Piacentini R.: *Improvement of the efficiency of a bare solar collector by means of turbulence promoters.* Appl. Energy **36**(1990), 4, 253–261.

[12] Webb R.L.: *Heat transfer and friction in tubes with repeated rib roughness.* Int J. Heat Mass Tran. **14**(1971), 4, 601–617.

[13] Varun, Saini R.P., Singal S.K.: *Investigation of thermal performance of solar air heater having roughness elements as a combination of inclined and transverse ribs on the absorber plate.* Renew. Energ. **33**(2008), 6, 1398–1405.

[14] Deo N.S., Chander S., Saini J.S.: *Performance analysis of solar air heater duct roughened with multigap V-down ribs combined with staggered ribs.* Renew. Energ. **91**(2016), 484–500.

[15] Kumar S.T., Mittal V., Thakur N.S., Kumar A.: *Heat transfer and friction factor correlations for rectangular solar air heater duct having $60°$ inclined continuous discrete rib arrangement.* Brit. J. Appl. Sci. Technol. **1**(2011), 3, 67–93.

[16] Bopche Santosh B., Tandale Madhukar S.: *Experimental investigations on heat transfer and frictional characteristics of a turbulator roughened solar air heater duct.* Int. J. Heat. Mass Tran. **52**(2009), 11–12, 2834–2848.

[17] Saini S.K., Saini R.P.: *Development of correlations for Nusselt number and friction factor for solar air heater with roughened duct having arc-shaped wire as artificial roughness.* Sol. Energy **82**(2008), 12, 1118–1130.

[18] ASHRAE Standard 93–77.: *Methods of testing to determine the thermal performance of solar collectors.* New York 1977.

[19] Holman J.P.: *Experimental Method for Engineers.* McGraw Hill. New York 2007.

[20] Hans V.S., Saini R.P., Saini J.S.: *Heat transfer and friction factor correlations for a solar air heater duct roughened artificially with multiple v-ribs.* Sol. Energy **84**(2010), 6, 898–911.

[21] Kumar D., Prasad L.: *Analysis on optimal thermohydraulic performance of solar air heater having multiple V-shaped wire rib roughness on absorber plate.* Int. Energy J. **18**(2018), 2, 153–170.

[22] Turkyilmazoglu M., Pop I.: *Heat and mass transfer of unsteady natural convection flow of some nanofluids past a vertical infinite flat plate with radiation effect.* Int. J. Heat Mass Tran. **59**(2013), 167–171.

[23] Fetecau C., Hayat T., Corina Fetecau.: *Steady-state solutions for some simple flows of generalized Burgers fluids.* Int. J. Non-linear Mech. **41**(2006), 8, 880–887.

[24] Liu X., Lienhard J.H., Lombara J.S.: *Convective heat transfer by impingement of circular liquid jets.* J. Heat Trans-T. ASME **113**(1991), 3, 571–582.

[25] Tong A.Y.: *A numerical study on the hydrodynamics and heat transfer of a circular liquid jet impinging onto a surface.* Numerical. Heat Tr. A-Appl. **44**(2003), 1, 1–19.

[26] Maithani R., Saini J.S.: *Heat transfer and friction factor correlations for a solar air heater duct roughened artificially with V-ribs with symmetrical gaps.* Exp.Therm. Fluid Sci. **70**(2016), 220–227.

[27] Layek A., Saini J.S., Solanki S.C.: *Second law optimization of a solar air heater having chamfered rib-groove roughness on absorber plate.* Renew. Energ. **32**(2007), 12, 1967–1980.

[28] Karmare S.V., Tikekar A.N.: *Heat transfer and friction factor correlation for artificially roughened duct with metal grit ribs.* Int. J. Heat Mass Tran. **50**(2007), 21–22, 4342–4351.

[29] Jaurker A.R., Saini J.S., Gandhi B.K.: *Heat transfer and friction characteristics of rectangular solar air heater duct using rib-grooved artificial roughness.* Sol. Energy **80**(2006), 8, 895–907.

[30] Tanda G.: *Performance of solar air heater ducts with different types of ribs on the absorber plate.* Energy **36**(2011), 11, 6651–6660.

[31] Lanjewar A., Bhagoria J.L., Sarviya R.M.: *Experimental study of augmented heat transfer and friction in solar air heater with different orientations of W-rib roughness.* Exp. Therm. Fluid Sci. **35**(2011), 6, 986–995.

[32] Fabbri M., Dhir V.K.: *Optimized heat transfer for high power electronic cooling using arrays of microjets.* J. Heat Trans-T. ASME **127**(2005), 7, 760–769.

[33] Muszyński T., KoziełS.M.: *Parametric study of fluid flow and heat transfer over louvered fins of air heat pump evaporator.* Arch. Thermod. **37**(2016), 3, 45–62.

[34] Robinson A.J., Schnitzler E.: *An experimental investigation of free and submerged miniature liquid jet array impingement heat transfer.* Exp. Therm. Fluid Sci. **32**(2007), 1, 1–13.

[35] Choo K., Friedrich B.K., Glaspell A.W., Schilling K.A.: *The influence of orifice-to-plate spacing on heat transfer and fluid flow of submerged jet impingement.* Int. J. Heat Mass Tran. **97**(2016), 66–69.